

Mesoporous Sulfonated Carbon Materials Prepared by Spray Pyrolysis

Nicolas Duyckaerts,^[a] Ioan-Teodor Troțuș,^[a] Valentina Nese,^[a] Ann-Christin Swertz,^[a] Sebastian Auris,^[a] Hartmut Wiggers,^[b] and Ferdi Schüth*^[a]

A one-step approach was developed for the production of mesoporous sulfonated carbon materials by means of an aerosol synthesis. Nebulizing a clear aqueous solution of sucrose and sulfuric acid through a heated oven leads to subsequent dehydration, carbonization and sulfonation of the carbohydrate structure, in less than two seconds residence time. Acid site concentrations ranging from 0.1 to 0.6 mmol g⁻¹ can be obtained. Porosity can easily be introduced via salt templating, and can be adjusted by varying the loading and type of salt

used. The highest surface area was obtained with Li₂SO₄, giving a BET surface area of 506 m² g⁻¹ and a mesopore size distribution between 2 and 8 nm. Fructose dehydration and inulin hydrolysis showed that the porous materials synthesized by salt templating are more active than the bulk ones, especially for inulin hydrolysis, for which the initial activity is enhanced by a factor of seven, making these materials competitive with the most active commercial resins.

Introduction

Sulfonated carbon materials are known for carrying strong sulfonic acid groups, potentially offering an alternative to the use of inorganic acids.^[1] They were often reported to have similar or superior activities to regular commercial acid resins, typically for biomass conversion.^[2] This class of materials were shown to be applicable in the field of adsorbents, ion-exchangers,^[3] lithium battery anodes,^[4] and fuel cells.^[5] Moreover, mesoporous carbon materials treated with acid also show advantages in metal dispersion after impregnation with metal salt solutions, due to the increased hydrophilicity of the support.^[6] Mesoporous carbon materials have also been used as templates, which are preferably low-cost and highly tunable.^[7]

Several synthesis strategies for sulfonated carbon materials were reported, leading to a wide variety of such materials. Two general approaches can be chosen: (1) carbon precursors are first sulfonated, followed by a partial carbonization,^[8] or (2) the carbonization step precedes the sulfonation step.^[9] In the first case, one-step syntheses have been developed, but making use of already sulfonated organic compounds. In the latter case, several forms of activated^[10] carbon materials and hard^[11]

or soft^[12] templated carbon materials have been sulfonated under different sulfonation conditions; also ordered mesoporous carbon materials^[13] and carbon composites were used as starting materials.^[14] Many of the mentioned systems are elegantly synthesized, and also for some of the systems excellent catalytic performance has been reported for different reactions. Therefore a simple, scalable production process for sulfonated carbon materials appeared to be highly attractive.

Such a process, leading to the formation of sulfonated carbon materials with controllable porosity, is described herein. Our technique makes use of sulfuric acid and an organic precursor, which are converted in one step to a catalytically active sulfonated carbon, with the added advantage that the surface area and porosity of the material can easily be tuned.

Aerosol-synthesis, or spray-pyrolysis, is a straightforward technique for the production of carbon materials.^[15] To the best of our knowledge, however, there are no reports on the preparation of sulfonated carbon materials by this route. With spray pyrolysis we were able to combine carbon formation, sulfonation, and salt templating in one step, leading to a simple and low-cost method for the direct synthesis of sulfonated carbon materials, offering texture and porosity control. To produce the materials, it is sufficient to nebulize an aqueous solution of sucrose and sulfuric acid into an aerosol, which is subsequently sent through an oven at elevated temperature. Evaporation of the water, dehydration of the carbohydrate structure, carbonization, and sulfonation take place in less than two seconds residence time.

[a] N. Duyckaerts, I.-T. Troțuș, V. Nese, A.-C. Swertz, S. Auris, Prof. Dr. F. Schüth
Heterogeneous catalysis
Max-Planck-Institut fuer Kohlenforschung
Kaiser-Wilhelm-Platz 1, 45470 Muelheim an der Ruhr (Germany)
E-mail: Schueth@kofo.mpg.de

[b] Dr. H. Wiggers
CeNIDE, Center for Nanointegration Duisburg-Essen
University of Duisburg-Essen
Carl-Benz-Str. 199, 47057 Duisburg (Germany)

Supporting information for this article is available on the WWW under <http://dx.doi.org/10.1002/cctc.201500483>.

This publication is part of a Special Issue on Carbon in the Catalysis Community. Once the full issue has been assembled, a link to its Table of Contents will appear here.

Results and Discussion

Functional groups and acidity

Functional groups of the synthesized carbon materials were qualitatively determined by attenuated total reflectance (ATR) infrared spectroscopy (Figure 1). The strongest absorptions

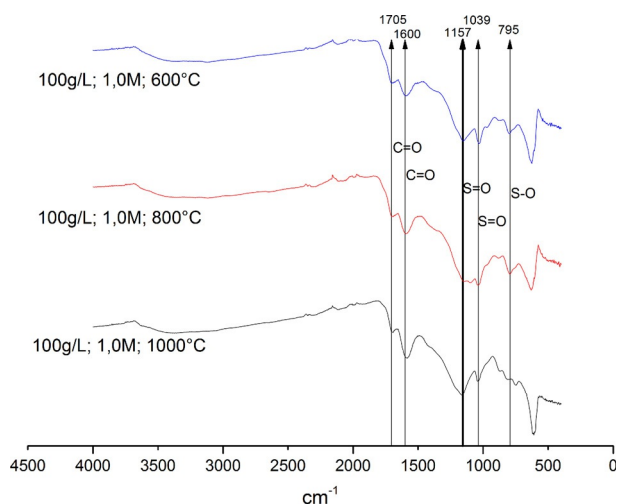


Figure 1. IR spectra of sulfonated carbon materials synthesized at various temperatures. Main peaks are qualitatively identified following literature values.^[16]

were identified based on literature values,^[16] of main importance is the broad absorption band at 1157 cm^{-1} attributed to $\text{S}=\text{O}$ stretching vibrations of sulfonic acid.

The total acidity was measured by HCl back-titration after stirring the material in a 0.1 M NaOH solution (50 mg in 10 mL), resulting in quantification of the sulfonic acid (strong acidity) together with possible carboxylic groups and acidic hydroxyls (weak acidity), which are all deprotonated at the high pH of the NaOH solution. The amount of strong acidity (sulfonic groups only) is given in terms of salt-splitting capacity, which can be seen as a measure of ion-exchange capacity (IEC). The salt-splitting capacity is measured by ion exchange of the sulfonated carbon materials in 1 M NaCl solution (50 mg in 10 mL) after which a known fraction of the supernatant (5 mL) is titrated with NaOH . In Figure 2 it is illustrated how these acidities vary with synthesis temperature; higher pyrolysis temperatures lead to a decrease in strong acidity and an even bigger decrease in weak acidity. This result already suggests a higher carbonization degree of the materials, as evident from the elemental analysis (see below).

During a synthesis of typically 2 h , the particles were trapped in a water bottle that reaches approximately 60°C by the heat of the carrier gas, bringing the synthesized material to an average contact time of 1 h with hot water. Afterwards, the material was rinsed extensively with water (20 L g^{-1}) during which neutrality of the filtrate is quickly reached as well as a negative barium sulfate test. This allows the conclusion that

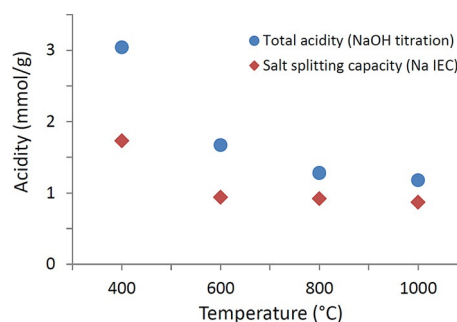


Figure 2. Total acidities determined by NaOH titration, comprising weak and strong acidic sites (blue). Salt-splitting capacities determined by Na ion exchange comprising strong acidic sites (red), for various synthesis temperatures.

after that treatment any residual free sulfuric acid has been removed.

However, sulfonated carbon materials are notorious for partly hydrolyzing and losing acidic groups under reaction conditions.^[8c, 10a, 12a, 17] For the carbon materials described here only approximately 45% of the strong acidity is prone to hydrolyze under aqueous conditions at high temperatures, whereas the other 55% shows stable catalytic activity. The hydrolyzed strong acidic groups can be more labile sulfonic groups ($\text{C}-\text{SO}_3-\text{H}$) but most probably less stable sulfate groups ($\text{C}-\text{OSO}_3\text{H}$), which hydrolyze more easily. The leaching behavior was investigated by performing a hydrothermal treatment at 120°C , which revealed that no further hydrolysis occurs after one hour of treatment, not even after prolonging the treatment up to seven days. The extent of acidity loss depends on the synthesis temperature, ranging from 40 to 50% for 400 to 800°C . The sulfonic acid of the material synthesized at 1000°C hydrolyzed to an extent of 82%, which leads to the conclusions that this temperature is not appropriate for the synthesis of a stable sulfonated carbon.

Energy-dispersive X-ray spectroscopy (EDX) of the cross section of a particle reveals uniform sulfur distribution throughout the carbon matrix (Figure 3), and elemental analysis of sulfur corresponds to the measured IEC before and after the hydrothermal leaching step (Table 1). The acidity measured through ion exchange is approximately 15% lower than the sulfur con-

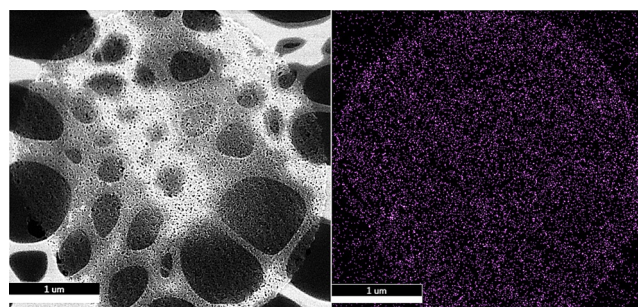


Figure 3. SEM image and corresponding sulfur elemental mapping of a microtome cross sections showing a homogeneous distribution of sulfur in a mesoporous carbon particle.

Table 1. Elemental analysis of carbon materials synthesized at various temperatures together with acidity content measured by ion-exchange. (synthesis conditions: sucrose 100 g L⁻¹, 1 M H₂SO₄)

T [°C]	C [wt%]	H	O	S	S ^[a] [mmol g ⁻¹]	Acidity ^[b]
400	52.91	3.70	39.82	3.57	1.12	1.41
400HT ^[c]	55.84	3.44	38.85	1.87	0.58	0.59
600	58.77	2.71	36.06	2.46	0.77	0.63
600HT ^[c]	60.02	4.54	34.07	1.37	0.43	0.60
800	63.13	3.11	31.87	1.89	0.59	0.49
800HT ^[c]	63.96	3.02	32.14	0.88	0.28	0.30
1000	70.00	3.55	25.05	1.40	0.44	0.41
1000HT ^[c]	71.61	2.75	25.37	0.27	0.08	0.12

[a] Determined by elemental analysis. [b] Determined by ion-exchange. [c] Hydrothermal hydrolysis step at 120 °C for 2 h.

tent, except for the materials sprayed at 400 °C, for which the IEC is 25 % higher. This could be attributed to the low synthesis temperature, resulting in a larger amount of weakly acidic groups (3 mmol g⁻¹), which could influence the IEC. As can be expected, the carbon content per mass increases with increasing pyrolysis temperature, whereas the oxygen and sulfur content decrease. The elemental analysis results permitted to calculate the overall production yield of this process, because the volume of liquid sent through the oven was known to be approximately 5 mL h⁻¹, and the amount of material obtained is 100 mg h⁻¹. The calculated carbonization yield is approximately 30 % with respect to the carbon content of sucrose, and the yield of sulfur incorporation is approximately 1.2 % for the sulfonated carbon materials synthesized at 800 °C. Thermogravimetric analysis in air confirmed that the higher carbonization extent results in an increased thermal stability of the carbon matrix (see the Supporting Information, Part 1).

Introducing porosity by salt templating

When a sucrose and sulfuric acid solution is sprayed, the droplets are carried through a heated section of a tube in which water begins to evaporate, sulfuric acid and sucrose become more and more concentrated and begin reacting. Through a series of dehydration, carbonization and sulfonation reactions, a bulk carbon material is obtained, with particle sizes ranging from 1 to 30 μm. Surface areas are approximately 2–3 m² g⁻¹. Scanning electron microscopy (SEM) analysis revealed that these particles mainly consist of broken hollow structures (Figure 4), which is typical for this synthesis method.^[15e,18] The high initial temperature gradients in the droplets make the carbonization start around the interface initiating hollow sphere formation, while the subsequent water evaporation leads to a rupture of the hollow structure.

Porosity can easily be generated by adding inorganic salts^[15d,19] to the clear starting solution. If a salt is present in the sprayed solution, it crystallizes in parallel with the above mentioned reactions and it therefore serves as a hard template, which is readily removed in the water trap. The micrographs in Figure 5 illustrate that the salt templating occurred uniformly throughout the carbon structure and the plots in Figure 6 depict to which extent the sodium sulfate loading de-

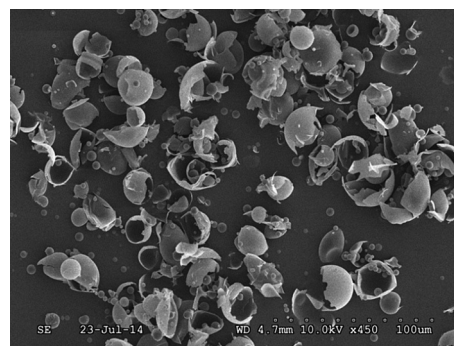


Figure 4. SEM picture of sulfonated carbon (sucrose 100 g L⁻¹, 1 M aqueous H₂SO₄, 800 °C).

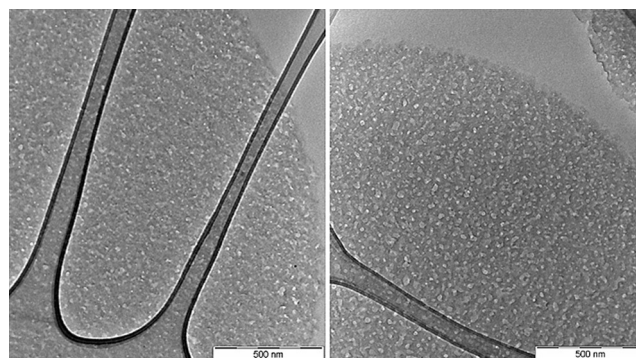


Figure 5. TEM images of microtome cross sections showing a homogeneous distribution of the mesoporous structure. (100 g L⁻¹ sucrose, 3 g Na₂SO₄ in 1 M H₂SO₄ solution; 600 °C left, 800 °C right)

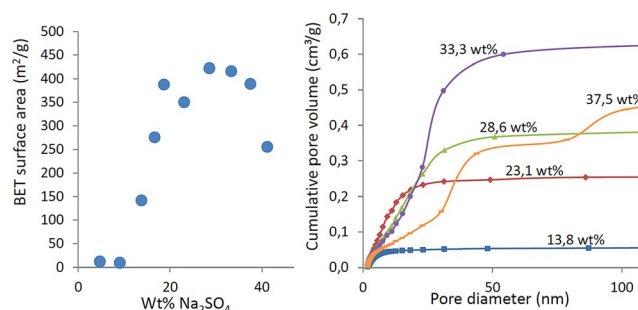


Figure 6. Effect of sodium sulfate loading (wt% towards sucrose) on the obtained BET surface (left) and the cumulative pore volume (right) for materials synthesized at 800 °C.

termines porosity. As seen in Figure 6, a plateau is reached at a surface area of 400 m² g⁻¹ between 18 and 38 wt% Na₂SO₄ loading, between which the pore diameter increases with loading, giving a maximum in measurable pore volume obtained at 33 wt%.

The salt-templated materials synthesized at 400 and 600 °C had much lower surface areas than those produced at 800 °C, probably as a result of collapse of the pores upon drying (Supporting Information, Part 2). When the salt templating was performed with sulfates having different cations at equal molar concentrations, different surface areas and pore size distribu-

tions were obtained (Supporting Information, Part 2). Interestingly, Li_2SO_4 templating led to a much narrower pore-size distribution (2–8 nm) than Na_2SO_4 and K_2SO_4 (2–25 nm) templating, leading to a lowered pore volume and higher surface area ($506 \text{ m}^2 \text{ g}^{-1}$). The use of sulfate salts lowers the sulfonation degree by approximately 15%, attributable to the lowered acidity in solution caused by the protonation of the sulfate ions to bisulfate. This lowered sulfonation, however, could be compensated by increasing the sulfuric acid concentration of the starting solution to restore initial acidities, which is consistent with the fact that the salt templating, regardless of the salt used, does not affect the sulfonation degree, as long as the pH is kept constant. The weak acidity however, is increased upon salt templating, by 20% for Na_2SO_4 and K_2SO_4 , and even by 240% for Li_2SO_4 at a synthesis temperature of 800°C (Supporting Information, Part 4). This phenomenon could be attributed to the decreased cross-linking at the interface of the salt crystals and the carbon matrix during synthesis, resulting in additional weakly acidic hydroxyl groups.

Insights into Fructose dehydration and inulin hydrolysis

Fructose dehydration to 5-hydroxymethylfurfural and subsequent hydrolysis to levulinic acid and formic acid, was used to investigate the activity of the sulfonated carbon materials in comparison with sulfuric acid and commercial acid resins (Figure 7). The type of commercial resin (Amberlyst 70) used

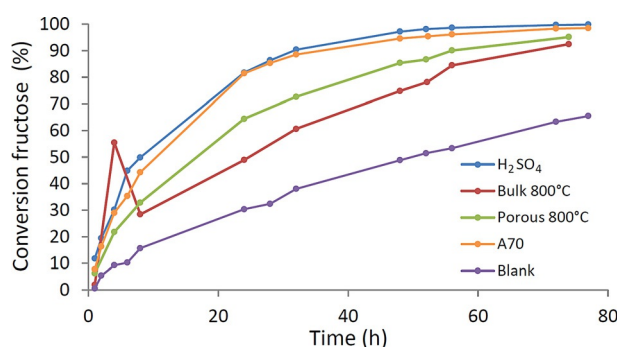


Figure 7. Conversion profile for fructose dehydration with various catalysts, fructose/acidity 25:1. (0.56 M fructose, 4 mol% acidic groups, 120°C , H_2O). The spike seen for the bulk material at short times has repeatedly been observed to different extent; see the Supporting Information.

for comparison in this paper, is the most active for fructose dehydration amongst three other Amberlyst resins tested (Supporting Information, Part 5). The sulfonated carbon materials synthesized at 800°C were selected for catalysis because of their high surface areas, combined with a higher carbonization degree, which leads to a higher observable structural stability in water ("bulk 800°C " refers to the material synthesized with 100 g L^{-1} sucrose in a 1 M H_2SO_4 solution, and "porous 800°C " was synthesized with additional 23.1 wt% Na_2SO_4). The carbon materials used for catalysis had all been hydrothermally treated at 120°C for 2 h and washed before catalysis, to ensure that all leachable species had been removed. For fructose dehydration,

sulfuric acid showed the highest activity, followed by Amberlyst 70, porous sulfonated carbon, bulk sulfonated carbon and the blank reaction (turnover frequency per hour: 2.9, 1.9, 1.5, 0.5, 0.1, respectively; calculated after 1 h reaction). Thus, the porous matrix provided by salt templating leads to an increase by a factor of three in initial reaction rate compared to the bulk carbon material, which can be explained by enhanced transport kinetics or improved accessibility of the active sites. Yields of 5-hydroxymethylfurfural, levulinic acid, and humins are shown in the Supporting Information (Supporting Information, Part 6).

Inulin hydrolysis to fructose and glucose was performed to investigate the activity of the materials in the conversion of bulkier substrates (Figure 8). Interestingly, the porous sulfonat-

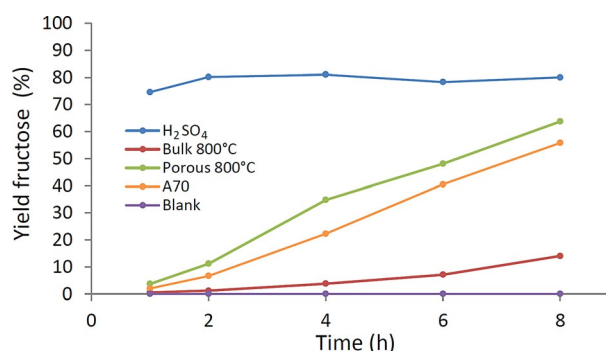


Figure 8. Yield of fructose from inulin hydrolysis, for various catalysts. (0.56 M fructose equivalents, 4 mol% acidic groups, 70°C , H_2O)

ed carbon material shows higher activity than Amberlyst 70, whereas the bulk sulfonated carbon material has inferior activity. This confirms again the positive influence of the porosity on mass transfer, which is more pronounced for bulkier reactants. For inulin, the induced porosity leads to an increase in initial activity by a factor of seven.

Conclusions

Stable mesoporous sulfonated carbon materials were obtained by a remarkably easy process. By nebulizing a clear aqueous solution of sulfuric acid, sucrose, and sodium sulfate through an oven, a mesoporous sulfonated carbon material was readily obtained within a remarkably short residence time of 2 s. As observed for different sulfonated carbon materials at varying extent, not all sulfonic acid groups were stable. Hydrothermal treatment at 120°C and autogenous pressure revealed that between 50 and 60% of the sulfonic groups are stable for several days under these conditions. The incorporation of porosity by salt templating had clear benefits in catalysis, increasing the initial reaction rate by 300% for fructose dehydration and by 700% for inulin hydrolysis, assumedly caused by the better accessibility and enhanced transport kinetics. The mesoporous sulfonated carbon materials therefore can compete with commercial acidic resins. In addition, the synthesis route is scalable and makes use of rather cheap starting materials. It also shows

that aerosol synthesis techniques are a versatile approach towards functionalized materials, promising further innovations.

Experimental Section

Material synthesis was performed using an in-house built spray pyrolyser, depicted in Figure 9. The ultrasonic atomizer nozzle (130 kHz) was purchased from Sonaer Ultrasonics. The nozzle holder was built in-house together with the trap whereas all remaining parts are standard equipment.

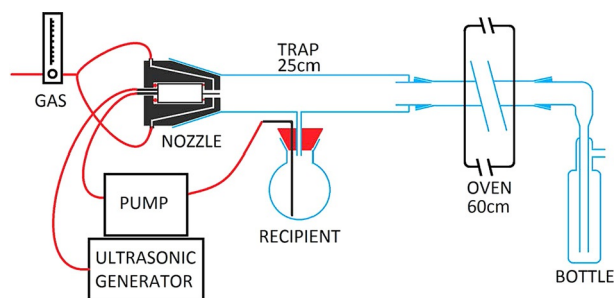


Figure 9. Schematic representation of the spray-pyrolysis setup.

The sulfonated carbon materials were synthesized from a clear solution of sucrose (50–300 g L⁻¹) in an aqueous sulfuric acid solution (0.5–2 M). For the mesoporous samples, sulfate salts were added (10–50 g L⁻¹). The clear solution was then pumped (7 mL min⁻¹) through the ultrasonic nebulizer. A nitrogen flow (1000 L h⁻¹) carried the aerosol through the oven (400–1000 °C), after which the formed particles were trapped in a water bottle. The collected particles were filtered on a glass frit (porosity 4) and subsequently washed with deionized water (20 L g⁻¹), and dried at 90 °C.

The catalytic tests were performed in a 20 mL glass vial starting from a 9 wt% and 5 wt% solution of fructose and inulin, respectively, in water. The catalyst amount added corresponded to a molar ratio of 25:1 of reactant to acid groups, determined by titration. The glass vial was then sealed with a septum and heated to the desired reaction temperature (120 °C for fructose dehydration and 70 °C for inulin hydrolysis). Samples were taken with a syringe.

Products were quantified by HPLC (Shimadzu LC-20), equipped with a column switch that combines a 100 and a 300 mm organic resin column of 8 mm ID. The eluent was an aqueous solution of trifluoroacetic acid (2 mM, 1 mL min⁻¹). The column temperature was 40 °C. Fructose and levulinic acid were analyzed using a RI detector, and 5-hydroxymethylfurfural was measured by using a UV detector. For fructose dehydration, the conversion was calculated as the ratio between the moles of reacted fructose (via a response factor) and the initial moles of fructose (mass of fructose used), and for inulin the conversion was calculated as a sum of the moles of identified products (via response factor) divided by the moles of fructose (equivalents of fructose in the mass of inulin used) introduced at the beginning of the reaction.

Electron microscopy and EDX mapping were performed on cross sections of the sulfonated carbon materials. For the preparation of the cross sections the samples were embedded in epoxy resin and cut by microtomy into approximately 50 nm thin slices. TEM

images were recorded with a Hitachi H-7100 Transmission Electron Microscope operated at 100 kV. STEM images and EDX analysis were performed on a Hitachi HD-2700 dedicated Scanning Transmission Electron Microscope operated at 200 kV equipped with an EDAX Octane T Ultra W EDX detector. IR spectroscopy was performed on an ATR diamond cell with a Nicolet Magna IR 560 spectrometer.

Nitrogen sorption analysis was performed with a Micromeritics ASAP 2000 instrument. Thermogravimetric analysis (Air, 10 °C min⁻¹) was performed with a Netzsch Jupiter STA 449 C. Elemental analysis was performed by: Chemical laboratory H. Kolbe, Mülheim/Ruhr.

Acknowledgements

The authors kindly thank Silvia Palm for the SEM analysis and discussion; Heike Hinrichs and Marie Sterling for the HPLC analysis and discussion; together with Andre Pommerin and Layla Sahraoui. Financial support by the ERC POLYCAT project is gratefully acknowledged.

Keywords: aerosol synthesis · fructose dehydration · salt templating · spray pyrolysis · sulfonated carbon

- [1] E. Lam, J. H. T. Luong, *ACS Catal.* **2014**, *4*, 3393–3410.
- [2] a) L. Geng, G. Yu, Y. Wang, Y. Zhu, *Appl. Catal. A* **2012**, *427–428*, 137–144; b) A. Onda, T. Ochi, K. Yanagisawa, *Top. Catal.* **2009**, *52*, 801–807; c) X. Mo, E. Lotero, C. Lu, Y. Liu, J. Goodwin, *Catal. Lett.* **2008**, *123*, 1–6; d) S. Suganuma, K. Nakajima, M. Kitano, H. Kato, A. Tamura, H. Kondo, S. Yanagawa, S. Hayashi, M. Hara, *Microporous Mesoporous Mater.* **2011**, *143*, 443–450.
- [3] A. K. Mittal, C. Venkobachar, *Ind. Eng. Chem. Res.* **1996**, *35*, 1472–1474.
- [4] Y. J. Kim, H. J. Lee, S. W. Lee, B. W. Cho, C. R. Park, *Carbon* **2005**, *43*, 163–169.
- [5] a) J. Tang, J. Liu, N. L. Torad, T. Kimura, Y. Yamauchi, *Nano Today* **2014**, *9*, 305–323; b) J.-B. Lee, Y.-K. Park, O. B. Yang, Y. Kang, K.-W. Jun, Y.-J. Lee, H. Y. Kim, K.-H. Lee, W. C. Choi, *J. Power Sources* **2006**, *158*, 1251–1255.
- [6] M. L. Toebe, F. F. Prinsloo, J. H. Bitter, A. J. van Dillen, K. P. de Jong, *J. Catal.* **2003**, *214*, 78–87.
- [7] W.-C. Li, A.-H. Lu, W. Schmidt, F. Schüth, *Chem. Eur. J.* **2005**, *11*, 1658–1664.
- [8] a) M. Hara, T. Yoshida, A. Takagaki, T. Takata, J. N. Kondo, S. Hayashi, K. Domen, *Angew. Chem. Int. Ed.* **2004**, *43*, 2955–2958; *Angew. Chem.* **2004**, *116*, 3015–3018; b) R. L. Johnson, J. M. Anderson, B. H. Shanks, K. Schmidt-Rohr, *Chem. Mater.* **2014**, *26*, 5523–5532; c) W. Zhang, H. Tao, B. Zhang, J. Ren, G. Lu, Y. Wang, *Carbon* **2011**, *49*, 1811–1820.
- [9] a) M. Okamura, A. Takagaki, M. Toda, J. N. Kondo, K. Domen, T. Tatsumi, M. Hara, S. Hayashi, *Chem. Mater.* **2006**, *18*, 3039–3045; b) M. Toda, A. Takagaki, M. Okamura, J. N. Kondo, S. Hayashi, K. Domen, M. Hara, *Nature* **2005**, *438*, 178–178.
- [10] a) X.-Y. Liu, M. Huang, H.-L. Ma, Z.-Q. Zhang, J.-M. Gao, Y.-L. Zhu, X.-J. Han, X.-Y. Guo, *Molecules* **2010**, *15*, 7188–7196; b) M. Kitano, K. Arai, A. Kodama, T. Kousaka, K. Nakajima, S. Hayashi, M. Hara, *Catal. Lett.* **2009**, *131*, 242–249; c) V. L. Budarin, J. H. Clark, R. Luque, D. J. Macquarrie, *Chem. Commun.* **2007**, 634–636.
- [11] J. Janaun, N. Ellis, *Appl. Catal. A* **2011**, *394*, 25–31.
- [12] a) I. Muylaert, A. Verberckmoes, J. Spileers, A. Demuyck, L. Peng, F. De Clippel, B. Sels, P. Van Der Voort, *Mater. Chem. Phys.* **2013**, *138*, 131–139; b) B. Chang, J. Fu, Y. Tian, X. Dong, *RSC Adv.* **2013**, *3*, 1987–1994.
- [13] a) R. Xing, Y. Liu, Y. Wang, L. Chen, H. Wu, Y. Jiang, M. He, P. Wu, *Microporous Mesoporous Mater.* **2007**, *105*, 41–48; b) L. Peng, A. Philippaerts, X. Ke, J. Van Noyen, F. De Clippel, G. Van Tendeloo, P. A. Jacobs, B. F. Sels, *Catal. Today* **2010**, *150*, 140–146; c) X. Wang, R. Liu, M. M. Waje, Z. Chen, Y. Yan, K. N. Bozhilov, P. Feng, *Chem. Mater.* **2007**, *19*, 2395–2397.

- [14] a) S. Van de Vyver, L. Peng, J. Geboers, H. Schepers, F. de Clippel, C. J. Gommès, B. Goderis, P. A. Jacobs, B. F. Sels, *Green Chem.* **2010**, *12*, 1560–1563; b) Y. Liu, J. Chen, J. Yao, Y. Lu, L. Zhang, X. Liu, *Chem. Eng. J.* **2009**, *148*, 201–206; c) Q. Yue, M. Wang, J. Wei, Y. Deng, T. Liu, R. Che, B. Tu, D. Zhao, *Angew. Chem. Int. Ed.* **2012**, *51*, 10368–10372; *Angew. Chem.* **2012**, *124*, 10514–10518.
- [15] a) Q. Hu, Y. Lu, G. P. Meisner, *J. Phys. Chem. C* **2008**, *112*, 1516–1523; b) J. H. Bang, K. Han, S. E. Skrabalak, H. Kim, K. S. Suslick, *J. Phys. Chem. C* **2007**, *111*, 10959–10964; c) Y. Yan, F. Zhang, Y. Meng, B. Tu, D. Zhao, *Chem. Commun.* **2007**, 2867–2869; d) M. E. Fortunato, M. Rostam-Abadi, K. S. Suslick, *Chem. Mater.* **2010**, *22*, 1610–1612; e) S. E. Skrabalak, K. S. Suslick, *J. Phys. Chem. C* **2007**, *111*, 17807–17811; f) J. Eric Hampsey, Q. Hu, L. Rice, J. Pang, Z. Wu, Y. Lu, *Chem. Commun.* **2005**, 3606–3608.
- [16] B. Schrader, *Nachr. Chem. Tech. Lab.* **1980**, *28*, 31–31.
- [17] a) J. M. Anderson, R. L. Johnson, K. Schmidt-Rohr, B. H. Shanks, *Carbon* **2014**, *74*, 333–345; b) X. Mo, D. E. López, K. Suwannakarn, Y. Liu, E. Lotero, J. G. Goodwin, Jr., C. Lu, *J. Catal.* **2008**, *254*, 332–338; c) J. M. Anderson, R. L. Johnson, K. Schmidt-Rohr, B. H. Shanks, *Catal. Commun.* **2014**, *51*, 33–36.
- [18] A. B. D. Nandiyanto, K. Okuyama, *Adv. Powder Technol.* **2011**, *22*, 1–19.
- [19] a) A.-H. Lu, W.-C. Li, W. Schmidt, F. Schüth, *Microporous Mesoporous Mater.* **2006**, *95*, 187–192; b) S. H. Kim, B. Y. H. Liu, M. R. Zachariah, *Langmuir* **2004**, *20*, 2523–2526.

 Received: May 4, 2015

Revised: July 6, 2015

Published online on August 25, 2015